Atomic Data Needs for X-ray Astronomy. 22 June 2000
http://heasarc.gsfc.nasa.gov/docs/heasarc/atomic/
M. A. Bautista, T. R. Kallman, and A. K. Pradhan, eds.

Coronal plasmas modeling and the MEKAL code

Jelle S. Kaastra and Rolf Mewe
SRON Laboratory for Space Research, Sorbonnelaan 2, 3584 CA Utrecht, The Netherlands

Abstract.
An overview is given of the current status of the spectral code development that takes place at SRON Utrecht.

1. A Short History

Starting in the early seventies (Mewe 1972) Rolf Mewe and his colleagues of the Space Research Laboratory in Utrecht started developing a spectral code for the X-ray emission of optically thin plasmas. A milestone was reached in 1985 and 1986, when two papers describing the line emission (Mewe et al. 1985) and continuum emission (Mewe et al. 1986) were published. This spectral code, often abbreviated as the Mewe-Gronenschild code, together with the Raymond & Smith code (1977) served for many years as the basis for many X-ray spectroscopic papers.

At the beginning of the eighties the code was extended with non-equilibrium ionization balance calculations (Gronenschild & Mewe 1982), and motivated by the work on supernova remnants done in Leiden by Fred Jansen and Jelle Kaastra vastly improved. The need for a faster code in order to be able to do spectral fitting to these non-equilibrium spectra of supernova remnants motivated us to improve the performance of the code. Then in 1992 an update of in particular the continuum calculation appeared, and this updated and faster computer code was implemented at HEASARC in the XSPEC package, at which time it was baptized as *meka* code, after the two main authors of this version, Mewe and Kaastra.

Around the same time we started the SPEX project, with the intention to improve, update and extend also the line emission part of the code. In addition we intended to make it more useful by having spectral simulation and fitting options attached to it, as well as more illustrative graphical and tabular output from the program, which helps to understand the physics of the sources being studied. Also different extensions like hydrodynamical models for supernova remnants, and differential emission measure analysis techniques were foreseen.

In 1994 the first version of SPEX became public, with the re-written *meka* code as working horse in the core of the software package. A year before the ASCA satellite had been launched, and in one of the first X-ray spectra of a cluster of galaxies, the Centaurus clusters, the observed spectrum did not match neither the predicted *meka* calculations nor the results of other codes like the Raymond & Smith code (Fabian et al 1994). In particular the ratio of the Fe-L blend from principal quantum level $n = 4$ to $n = 2$ as compared to the blend from from principal quantum level $n = 3$ to $n = 2$ did not match the observations. Around the same time, Duane Liedahl was able to produce better results for the Fe-L complex using the HULLAC atomic code, and by joining forces an update of the *meka* code, now named *mekal*, after the three authors, was released (Mewe, Kaastra & Liedahl 1995). This code was both included in the SPEX package as well as a model in the XSPEC package. Apart form the update and extension of the iron L complex, it also contained an improvement of the 300–2000 Å band, triggered by the EUVE spectra of stellar coronae, an update for the Fe VIII to Fe XVI ions, plus the addition of DR satellites for Mg XI. Also the ionization balance for iron was updated using the results of Arnaud & Raymond (1992).

The need for higher accuracy triggered us to try to update the code in a systematic way, working along isoelectronic sequences. The most recent developments in this work are described in the next sections.

2. Wavelength update

The grating spectrometers aboard of Chandra and XMM have a spectral resolution of 0.01–0.05 Å. However, for strong lines the line centroid can be determined much more accurately than the spectral resolution, if systematic wavelength errors can be taken out. Any uncertainties or rounding-off errors in the wavelengths of these lines as used in the spectral code will therefore lead to a significant mismatch of the predicted spectrum as compared to the observed spectrum. Only for the Sun X-ray spectra with such a high spectral resolution have been obtained with good statistics. Therefore using high-resolution solar flare X-ray spectra obtained with the Bragg Flat Crystal Spectrometer (FCS) on SMM, the lines of the *mekal* code in the 5–20 Å band were benchmarked (Phillips et al. 1999). Laboratory measurements of the wavelengths of these lines were also used to confirm the SMM values as well as published identifications from the HULLAC atomic code. The adjustments needed were up to 0.035 Å for line wavelengths above 13 Å but much less at shorter wavelengths. Although these corrections are small in an absolute sense, they are well detectable with Chandra and XMM. The wavelength corrections have been implemented now in the SPEX code.

3. Update of the atomic parameters

The update of our spectral code has two major branches: the ionization balance and the line/continuum formation. Recently, an update of the recombination rates for all ions from H–Ni has been given (Mazzotta et al 1998). Current work by us and Mazzotta on a similar update of the ionization rates is in progress.

In our update of the energy levels and oscillator strengths, we have now finished our systematic survey from the H-sequence up to the Al-sequence. These data are taken from the literature or lacking data, from the Cowan code.

Collision strength (both for proton and electron excitation) are collected from different sources and are fitted up to the Co-sequence. A considerable fraction of the collision strengths found in the literature is based upon the work of Zhang & Sampson and co-workers. The other part of our collision data originates from HULLAC calculations. Both the calculated data and the data gathered from literature are then fitted by a simple formula:

$$\Omega(U) = \sum_{i=0}^{6} \frac{c_i}{(U+s)^i} + c_7 \ln U + \sum_i a_i \delta(U - U_i), \tag{1}$$

where $U \equiv E/E_{\rm ex}$ with E the energy of the incoming electron and $E_{\rm ex}$ the excitation energy of the transition. The constants $c_0 \ldots c_7$ and s are free parameters, but are forced to be zero for some transitions, e.g., spin-forbidden transitions have $c_0 = c_1 = c_7 \equiv 0$. Further, if resonances are available these can be approximated by the terms with a_i and U_i: for most applications we do not need to know the deatiled resonance structure, but only its integral over some broad electron distribution. To that purpose, nearby resonances can be lumped together, and only their total strength a_i and average energy $U_i E_{\rm ex}$ needs to be given. In practice, no case required more than effectively four resonance terms.

The advantage of Equation (1) is that it can be integrated analytically for a Maxwellian energy distribution, as well as for a power law distribution. For other distributions, the integration can be done numerically. Some other schemes have been proposed where either the scaled collision strength is calculated using splines or a (spline) approximation is made to the Maxwellian-averaged collision strength. Although this is quite useful for thermal electron distributions, it causes difficulties when other electron distributions are considered, since then one needs to go back to the original collision strengths.

The fitting of the data in the literature or from HULLAC calculations to Equation (1) is done to either the original collision strengths, the Maxwellian averaged rates or both, depending upon what is provided in the original publication or data set. Examples of these fits can be found in Mewe (1999).

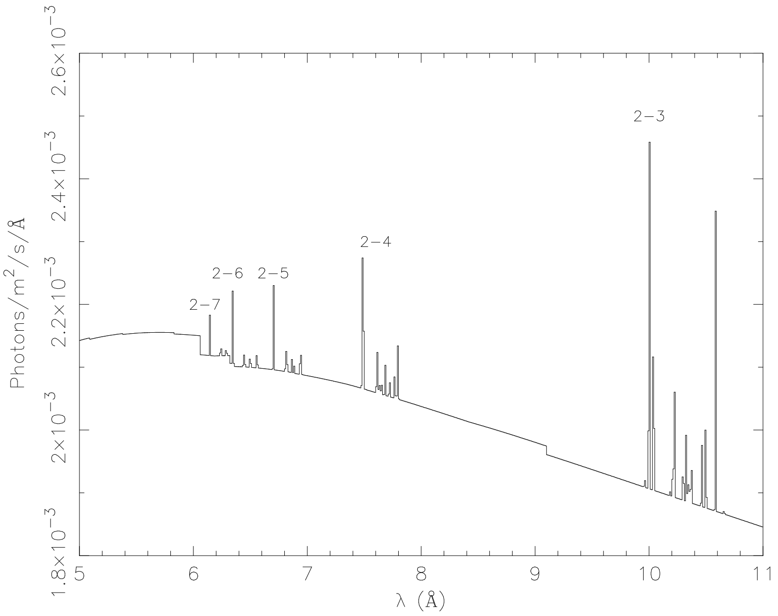

Figure 1. Newly calculated X-ray spectrum of Fe XXV for a temperature of 3 keV.

4. Preliminary results

Although much of the work on validation and implementation of these updated atomic parameters is still in progress, we report here some particular results.

Even for an isoelectronic sequence that is considered to be quite simple, our new results show significant differences with the old *mekal* calculations. For example, in the hydrogenic isoelectronic sequence, the newly calculated Lyman α line power differs in most cases no more than 10 % from the older calculations. But for the higher transitions, like Lyman β, Lyman γ of Hα the differences can be larger tahn 50 %. An illustration can be found in Kaastra (1998).

Here we show some results for He-like ions. Figure 1 shows our new calculations for Fe XXV. We took a temperature of 3 keV. The spectrum shown consists of the complete continuum of all elements, but for the line emission we have selected only the Fe XXV lines. Only the (dominant) excitation contributions to the line formation have been taken into account. The collision rates are based upon Sampson et al. (1983) and Zhang & Sampson (1987). The plot shows the complete spectrum in the Fe-L band, including all transitions up to $n = 7$. In this wavelength range, the old *mekal* code only had 3 lines, and 9 lines in total for all wavelengths. Our present model has 494 lines.

5. Response matrices

One of the powerful features of SPEX is that it is also possible to do spectral simulation and fitting with the same package that calculates the atomic and hydrodynamical models. In general, spectral fitting is done by calculating a model spectrum on a discrete energy grid, folding this through the instrument response by multiplying the model spectrum by the response matrix, and optimizing the parameters of the model spectrum until agreement with the observed spectrum has been reached. This procedure works well with low- to medium resolution spectra, but yields difficulties when high-resolution spectra are analysed. The reason is that in high-resolution spectra the number of model bins becomes very large, in particular for line spectra, since the model spectrum needs to be sampled on a much finer grid than the observed spectrum (in particular for strong lines). Now most grating spectrometers have a rather narrow linespread function, but in addition there is a weaker but broad instrumental scattering

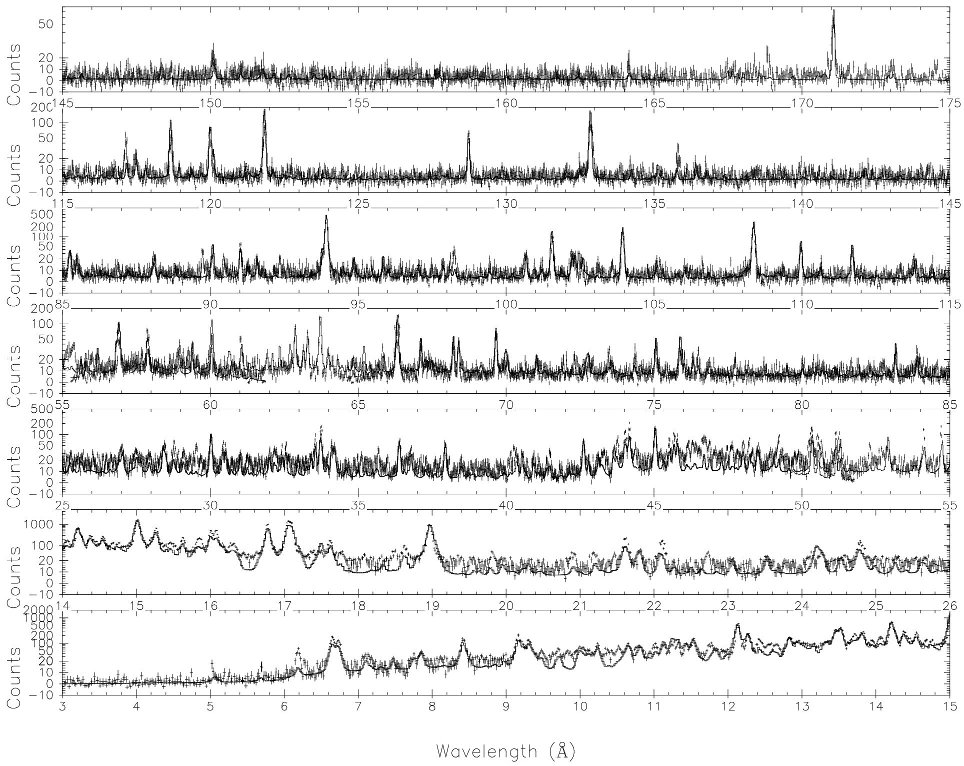

Figure 2. Chandra LETGS spectrum of Capella - both positive and negative spectral orders are plotted as crosses, the best fit model (see text) as solid lines.

component below the main peak. This scattering component in combination with the large number of model bins causes the response matrix to be untractably large.

There is a way out, however, if the following two steps are teken. First, in the classical treatment of response folding, the model spectrum is evaluated by defining an energy grid, and calculating the total number of photons in each individual bin of the grid. Thereby all information on the energy distribution of the photons within the bin is lost, and hence the effective energy resolution of the model is determined by the bin width of the grid. For strong lines, however, the average energy of the photons can be determined much more accurately than the bin width, it is essentially given by the rms width of the line spread function, divided by the square root of the number of photons. The natural way out of the binning problem is to take wider bins, for which not only the total number of photons is calculated, but also the average energy of all phtons within the bins. Taking both these numbers consistently into account in the convolution with the response matrix yields accurate results, with a significant reduction in computation time and energy grid size. The second important step is to split up the response matrix in as many components as are required for the line-spread function (lsf). For example, with the RGS spectrometer of XMM the lsf consists of a narrow core and a broad scattering wing. The model spectrum can be convolved with both components separately, and the predicted spectra should be combined at that stage. The reason is that the core of the lsf is narrow and needs a high-resolution energy grid for optimal accuracy, but since it is narrow and has no extended wings the corresponding response matrix is rather sparse. On the other hand, the scattering wings are broad and therefore do not need to be sampled on a very high-resolution grid; a coarser grid is sufficient, and in this way the corresponding response matrix also becomes manageable.

All this has been implemented now in the SPEX package, and in the next section we give an example of its use.

6. The Capella spectrum

We have applied our methods to the Chandra LETGS spectrum of Capella. We binned both the data and model energy grid optimally. The model energy grid had 40000 bins. The observed spectrum had 10 252 bins, the final response matrix contained 11 spectral orders, splitted into a narrow and broad response component, the total number of non-zero response elements was 7 335 000. Without the tricks and methods of the previous section, the size of the matrix would have been an order of magnitude larger. We fitted the spectrum using the *mekal* model with three isothermal components (0.04, 0.2 and 0.53 keV) and solar abundances. This fit is only illustrative, however. A preliminary analysis shows that the abundances deviate somewhat from the solar values, and agree more or less with what Brickhouse et al (2000) derived based upon the EUVE/ASCA data. It should have also been taken into account that the wavelength and efficiency calibration of the LETGS are not yet completely available, and this may also contribute partly to the large reduced χ^2 of the fit (about 4). We hope to improve this later by using the proper calibration as soon as it is available. Also, it should be noted that the fitting was done using the old *mekal* code; we expect that when our updated SPEX code is finished we will also obtain a better agreement.

Acknowledgments. The Laboratory for Space Research Utrecht is supported financially by NWO, the Netherlands Organization for Scientific Research.

References

Arnaud, M., Raymond, J., 1992, ApJ 398, 394

Brickhouse, N.S., Dupree, A.K., Edgar, R.J., et al., 2000, ApJ 530, 387

Burgess, A., Tully, J.A., 1992, A&A 254, 436

Fabian, A.C., Arnaud, K.A., Bautz, M.W., Tawara, Y., 1994, ApJ 436, L87

Gronenschild, E.H.B.M., Mewe, R., 1982, A&A Supp 48, 305

Kaastra, J.S., 1998, in: The hot universe, IAU Symp. 188, p. 43, eds. K. Koyama et al., Kluwer

Mazzotta, P., Mazzitelli, G., Colafrancesco, S., Vittorio, N., 1998, A&A Supp. 133, 403

Mewe, R., 1972, Solar Phys. 22, 459

Mewe, R., Gronenschild, E.H.B.M., van den Oord, G.H.J., 1985, A&A Supp 62, 197

Mewe, R., Lemen, J.R., van den Oord, G.H.J., 1985, A&A Supp 65, 511

Mewe, R., Kaastra, J.S., Liedahl, D.A., 1995, Legacy 6, 16

Mewe, R., 1999, in: X-ray spectroscopy in astrophysics, p. 109, eds. van Paradijs, J. & Bleeker, J.A.M., Springer.

Phillips, K.J.H., Mewe, R., Harra-Murnion, L.K., et al., 1999, A&A Supp. 138, 381

Raymond, J.C., Smith, B.W., 1977, ApJ Supp. Ser. 35, 419

Sampson, D.H., Goett, S.J., Clark, R.E.H., 1983, ADNDT 29, 467

Zhang, H., Sampson, D.H., 1987, ApJ Supp. Ser. 63, 487